

MICROPHONIC DETUNING INDUCED COUPLER KICK VARIATION AT LCLS-II

Thorsten Hellert*, DESY, Hamburg, Germany

Wolfgang Ackermann, Herbert De Gerssem, TU Darmstadt (TEMF), Darmstadt, Germany

Chris Adolphsen, Zenghai Li, Chris Mayes, SLAC, Menlo Park, CA 94025, USA

Abstract

The LCLS-II free-electron laser will be an upgrade of the existing Linac Coherent Light Source (LCLS), including a 4 GeV CW superconducting linac based on the TESLA technology. The high quality factor of the cavity makes it very sensitive to vibrations. The shift of its eigenfrequency (i.e., detuning) will be compensated by the power source in order to assure a constant accelerating voltage. Significant variations of the forward power are expected which result in coupler kick variations induced by the fundamental power coupler. In this work we estimate the magnitude of trajectory jitter caused by these variations. High precision 3D field maps including standing and traveling-wave components for a cavity with the LCLS-II coupler design are presented.

INTRODUCTION

The LCLS-II [1] free-electron laser will be an upgrade of the existing Linac Coherent Light Source (LCLS) [2], including a 4 GeV superconducting linac based on TESLA [3] technology. It is designed to deliver high average brightness beams with up to 1 MHz repetition rate in continuous wave (CW) operation.

The TESLA cavity is a 9-cell standing wave structure whose fundamental TM π -mode resonates at 1.3 GHz. It is equipped with a higher order mode (HOM) coupler at each end of the cavity [4] in order to extract undesired field excitations. The fundamental power coupler (FPC) connects the cavity to its power source and is mounted horizontally at the downstream end of the cavity.

The LCLS-II linac consists of 280 TESLA-style cavities with TTF-3 power couplers that are modified for CW operation with input powers up to about 7 kW [5]. The cavities are operated with a loaded quality factor $Q_L = 4.1 \times 10^7$.

Each TESLA cavity at LCLS-II is powered by its own 3.8 kW solid state amplifier (SSA) [6]. Considering CW operation, the effects of Lorentz force detuning and beam loading [7] are not expected to have a notable impact on adjacent bunches. However, the high quality factor of the cavity makes it very sensitive to vibrations, which shift the resonance frequency by about 300 Hz/ μm [8] of longitudinal deformation.

Cavity resonance control is provided by both a slow stepper motor and a fast piezo tuner. Residual microphonic detuning is expected to be a maximum of 10 Hz peak detuning [6] with rms value of $\Delta f_{\text{rms}} = 1.7$ Hz. Fast cavity field

control of the amplitude and phase of the accelerating field is specified to be 0.01 % and 0.01°.

Given the 32 Hz cavity bandwidth with $Q_L = 4.1 \times 10^7$ and a maximum microphonic detuning of 10 Hz, the forward power of the SSA has to be varied significantly (± 20 %) in order to achieve the tight specifications for the cavity fields. This leads to significant variations of the ratio between the forward and backward traveling waves in the FPC. The transverse fields induced by the FPC depend on this ratio [9], thus detuning related coupler kicks will vary along the bunch train.

In this paper we estimate the resulting beam jitter. Regarding the injector module, tracking is performed, whereas a discrete coupler kick model is used for the main linac. High precision 3D field maps including standing and traveling-wave components for a cavity with the LCLS-II loaded quality factor setup are presented and used for the field calculations.

FIELD MAP CALCULATIONS

For the current work the focus is to model the effects on the beam due to the cavity π -mode field and that due to both the two HOM couplers and the single FPC. Due to the geometric complexity of the structure the required calculation is based on a suitable numerical approach since exact analytical results are not feasible.

Suitable software has been developed in C++, which is able to provide the resonance frequency and quality factor for a certain number of modes as well as appropriate 3D field maps. The generated field maps represent complex-valued vector components for the electric field strength and the magnetic flux density at arbitrary sample points within the computational domain. From the many available methods, we concentrate for this particular kind of application on the finite element method (FEM) featuring higher-order vector-valued basis functions on curved tetrahedral elements.

Unfortunately, the available high flexibility of the unstructured mesh is inevitably associated to field fluctuations due to the inherent coupling of the individual field components within each computational element. The huge longitudinal field component of the electric field strength which is characteristic for the calculated π -mode generates artificial transverse field components. Because of the disordered arrangement of the computational elements, the extracted field components look noisy although the underlying origin is based on a deterministic process only.

According to Ref. [10] we apply a physically-motivated smoothing process based on the vector equivalents of the Kirchhoff integral. The proposed technique provides smooth

* thorsten.hellert@desy.de

fields within the entire computational domain without a classical suppression of high frequency field components based on elaborate filter techniques. All calculations are based on complex arithmetic to take into consideration the loss mechanism of the attached couplers. To simplify the huge computational task, the surface of the superconducting cavities is modeled with perfect electric conductive (PEC) material. Nevertheless, a locally bounded energy absorption through the waveguide port at the main coupler leads to a small net power flow within the entire resonator such that the complex-valued electro- magnetic field components have to be determined with a certain accuracy. The assembled nonlinear matrix pencil is finally solved by means of a fixed-point iteration within a linear Jacobi-Davidson (JD) method where the termination criterion for the iterative procedure has to be adopted to the specific needs. The entire solver finally provides a sufficient accurate numerical model to determine the eigenvalues and eigenvectors of the underlying eigensystem formulation.

There are different field maps available in Ref. [11], which are calculated for different penetration depths of the coaxial antenna of the FPC. This reflects different values of the loaded quality factor of the cavity. The field maps are given as a table of sine- and cosine-dependent amplitudes, $\vec{E}_b^{\sin}(\vec{r})$ and $\vec{E}_b^{\cos}(\vec{r})$, respectively for a decaying eigenmode with a backward traveling wave from the cavity into the waveguide on a defined grid $\vec{r}_i = [x, y, z]_i$. The overall electric field strength \vec{E} and magnetic flux density \vec{B} for the general case with accelerating voltage V_0 and phase ϕ with respect to the beam can be calculated as [9]

$$\begin{aligned} \vec{E}(\vec{r}, t) &= \Re \left[V_0/V_n e^{i(\omega t + \phi)} \cdot \left(E_b^{\cos} - i \Gamma \cdot E_b^{\sin} \right) \right] \\ \vec{B}(\vec{r}, t) &= \Re \left[V_0/V_n e^{i(\omega t + \phi)} \cdot \left(\Gamma \cdot \vec{B}_b^{\cos} + i \vec{B}_b^{\sin} \right) \right], \end{aligned} \quad (1)$$

where the quantity V_n normalizes the field to the Eigenmode solution of the field map and ω is the angular frequency of excitation. The parameter $\Gamma = (\mathbf{V}_b - \mathbf{V}_f)/(\mathbf{V}_b + \mathbf{V}_f)$ describes the ratio between the difference and sum of forward and backward waves from/to the FPC. The bold letters indicate complex numbers, for example $\mathbf{V}_b = V_b \cdot e^{i\phi_b}$.

Due to the high quality factor of the TESLA cavity, wall losses can be neglected. The ratio Γ is therefore determined by the amount of beam loading and the detuning of the cavity. For a superconducting cavity operating close to the steady state condition, nearly on crest and a detuning Δf small compared to the resonance frequency f_0 , the parameter Γ follows from the cavity voltage \mathbf{V}_0 as [12],

$$\Gamma = \frac{\mathbf{V}_b - \mathbf{V}_f}{\mathbf{V}_b + \mathbf{V}_f} = -\frac{R_L \mathbf{I}_B}{\mathbf{V}_0} + i \frac{2 Q_L}{f_0} \Delta f \quad (2)$$

with $\mathbf{I}_B = 2 I_{B0} e^{i\phi_B}$ being the beam current, I_{B0} the dc beam current and R_L the shunt impedance.

DISCRETE COUPLER KICKS

The principle idea of discrete coupler kicks (DCK) [13] is to describe the impact of the transverse forces induced by

the couplers onto the beam by discrete kicks at the coupler positions. The derivation of DCK has been described in detail in Ref. [9], a brief summary follows.

The coupler kick can be calculated as $\vec{k}(x, y) = e V_0/E_0 \cdot \Re \{ \tilde{\mathbf{V}}(x, y) \cdot e^{i\phi_0} \}$ from the amplitude V_0 and phase ϕ_0 of the cavity voltage, the beam energy E_0 and the normalized complex kick factor $\tilde{\mathbf{V}}(x, y) = (\mathbf{V}_\perp(x, y) - \mathbf{V}_{\text{RZ}}(r))/V_\parallel$, with the integrated transverse $\mathbf{V}_\perp(x, y) = \int dz \left[\vec{E}_\perp(\vec{r}) + c \vec{e}_z \times \vec{B}(\vec{r}) \right] e^{i \frac{\omega z}{c}}$ and longitudinal $\mathbf{V}_\parallel = \int dz \vec{e}_z \cdot \vec{E}(0, 0, z) e^{i \frac{\omega z}{c}}$ field acting on an ultra-relativistic paraxial particle. The axially symmetrical RF focussing part of the field, \mathbf{V}_{RZ} , can be calculated by evaluating the transverse field strength and extracting the monopole part. By taking the field map Eqs. (1) into account, the normalized complex kick factor for the general case of an arbitrary Γ can be written as $\tilde{\mathbf{V}} = \tilde{\mathbf{V}}^{\text{SW}} + \Gamma \cdot \tilde{\mathbf{V}}^\Gamma$, where $\tilde{\mathbf{V}}^{\text{SW}} = (\tilde{\mathbf{V}}^f + \tilde{\mathbf{V}}^b)/2$ and $\tilde{\mathbf{V}}^\Gamma = (\tilde{\mathbf{V}}^f - \tilde{\mathbf{V}}^b)/2$ are the field integrals of the sum and the difference of the forward and backward traveling waves, respectively. Only the fields related to the reflection dependent part $\tilde{\mathbf{V}}^\Gamma$ depend on the parameter Γ . For the fields that extend into the upstream beam pipe $\tilde{\mathbf{V}}^\Gamma \approx 0$.

It is useful to linearize the normalized complex kick factor $\tilde{\mathbf{V}}$ around the cavity axis. The zeroth and first order kick on a bunch induced by a coupler can be expressed as

$$\vec{k}(x, y) \approx \frac{e V_0}{E_0} \Re \left\{ \left[\begin{pmatrix} \mathbf{V}_{0x} \\ \mathbf{V}_{0y} \end{pmatrix} + \begin{pmatrix} \mathbf{V}_{xx} & \mathbf{V}_{xy} \\ \mathbf{V}_{yx} & \mathbf{V}_{yy} \end{pmatrix} \begin{pmatrix} x \\ y \end{pmatrix} \right] e^{i\phi} \right\}, \quad (3)$$

where x and y are the bunch horizontal and vertical offset at the coupler position. From the Maxwell's equations it follows that $V_{yy} = -V_{xx}$ and $V_{xy} = V_{yx}$. Thus, coupler kicks are up to first order well described with four normalized coupler kick coefficients $[\mathbf{V}_{0x}, \mathbf{V}_{0y}, \mathbf{V}_{xx}, \mathbf{V}_{xy}]$.

The coupler kick coefficients depend on the position of the power input antenna, thus the loaded quality factor of the cavity. For $Q_L = 4.1 \times 10^7$ the coefficients of $\tilde{\mathbf{V}}^\Gamma$ can be interpolated as $[\mathbf{V}_{0x}^\Gamma, \mathbf{V}_{0y}^\Gamma, \mathbf{V}_{xx}^\Gamma, \mathbf{V}_{xy}^\Gamma] = [-1.22 - 2.77i, 0.01 + 0.01i, 0.06 + 0.13i, 0.00 + 0.00i]$ [9].

From Eq. (2) it follows that for a given accelerating gradient and beam current, the variation $\Delta\Gamma$ and the detuning Δf are related as $\Delta\Gamma(\Delta f) = i 2 Q_L / f_0 \cdot \Delta f$. The horizontal zeroth order coupler kick variation which is related to the reflection dependent part is then given by

$$\Delta k_x^0 = \frac{e V_0}{E_0} \Re \{ \Delta\Gamma \cdot V_{0x}^\Gamma \cdot e^{i\phi} \} \quad (4)$$

Thus, for $Q_L = 4.1 \times 10^7$ and $\phi = 0^\circ$ it follows that $\Delta k_x^0 = e V_0/E_0 \cdot 0.176 \mu\text{rad}/\text{Hz}$, which results, for example, in a coupler kick variation of about 29 nrad for a cavity with $V_0 = 20 \text{ MV}$, beam energy of $E_0 = 120 \text{ MeV}$ and a detuning of $\Delta f = 1 \text{ Hz}$.

The coupler kick coefficients for the third harmonic cavities with $Q_L = 2.7 \times 10^7$ are calculated by assuming the same scaling as for the 1.3 GHz cavities (cf. Eq. (18) in Ref. [9]) as $[\mathbf{V}_{0x}^\Gamma, \mathbf{V}_{0y}^\Gamma, \mathbf{V}_{xx}^\Gamma, \mathbf{V}_{xy}^\Gamma] = [-5.72 + 6.45i, 0.37 - 0.23i, 0.38 + 0.36i, 0.06 + 0.05i]$.

COUPLER KICKS AT LCLS-II

In this section the magnitude of the trajectory variations that are caused by microphonic cavity detuning related coupler kick variations at LCLS-II are calculated. For each cavity a random detuning with a Gaussian distribution with Δf_{rms} is generated, while the accelerating gradient is assumed to be constant. The rms cavity detuning Δf_{rms} is subsequently increased from 0 Hz to 5 Hz. At each step, 10^4 detuning seeds are evaluated. For each detuning seed the corresponding trajectory is compared to the trajectory with zero detuning in all cavities. The relative trajectory jitter $\delta J = \sqrt{\bar{J}}/\epsilon$ is calculated with the mean action \bar{J} and the transverse emittance ϵ . No misalignments are considered.

Injector module: In the LCLS-II injector [15] the electrons are generated in a CW normal-conducting gun and injected into a ILC-style cryomodule at a beam energy of 0.75 MeV. Eight cavities accelerate the beam to a final energy of about 100 MeV. In this energy range the ultra-relativistic assumption is poorly satisfied. In order to calculate the trajectory jitter tracking is performed. Bunches are simulated as single particles.

With the RF parameters [16] and the parameter Γ as obtained by Eq. (2), the proper field map can be calculated via Eq. (1). We use a field map [11] with $Q_L = 4.59 \times 10^7$. The bunch charge is assumed to be 300 pC and $(R/Q) = 1010 \Omega$. A Runge-Kutta algorithm is then used to solve the equation of motion through the injector module for a particle which enters the module on axis. The rms trajectory differences at $\Delta f_{\text{rms}} = 1.7$ Hz are $[\Delta x, \Delta x', \Delta y, \Delta y']_{\text{rms}} = [0.56 \mu\text{m}, 0.14 \mu\text{rad}, 14 \text{ nm}, 3 \text{ nrad}]$. The horizontal relative trajectory jitter at the end of the module is well described as $\delta J(\Delta f_{\text{rms}}) = 0.95 \text{ \%}/\text{Hz} \cdot \Delta f_{\text{rms}}$.

SCRf linac: The LCLS-II linac consists of 35 ILC-style cryomodules, each housing eight TESLA cavities. The beam is accelerated from 100 MeV to 4 GeV, thus an energy range in which the ultra-relativistic assumption is a reasonable approach.

The effect of trajectory jitter caused by detuning-related coupler kick variations is estimated as follows. The LCLS-II design lattice [16] is used in order to calculate the transfer matrices [17] between the end of the cavities. After each cavity, a discrete downstream coupler kick is applied. With the RF parameters obtained by Eq. (2) with a random detuning Δf_{rms} , the coupler kicks are calculated for each bunch and each cavity individually and the beam transport through the accelerator is evaluated. The relative horizontal trajectory jitter at the end of the linac is plotted in Figure 1 and is well described as $\delta J(\Delta f_{\text{rms}}) = 1.23 \text{ \%}/\text{Hz} \cdot \Delta f_{\text{rms}}$.

Start-to-end: Trajectory jitter caused by all cavities is considered in a start-to-end calculation, including the injector module and 16 third harmonic cavities [18]. As described above, tracking is performed in the injector module while discrete coupler kicks are evaluated for other cavities. The relative horizontal trajectory jitter at the end of the main linac is well described as $\delta J(\Delta f_{\text{rms}}) = 1.54 \text{ \%}/\text{Hz} \cdot \Delta f_{\text{rms}}$. Including third harmonic cavities, the final jitter scales as

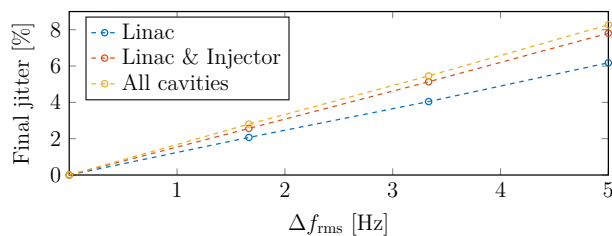


Figure 1: Tracking results for the trajectory jitter caused by detuning related coupler kick variations in LCLS-II. Plotted is the final beam jitter as a function of maximum detuning Δf_{rms} for the main linac (blue), the main linac and the injector module (red) and all cavities including the main linac, injector module and the 3.9 GHz cavities (yellow).

$\delta J(\Delta f_{\text{rms}}) = 1.66 \text{ \%}/\text{Hz} \cdot \Delta f_{\text{rms}}$, where Δf_{rms} is the detuning in the 1.3 GHz cavities. Note that 1 Hz microphonic detuning in 1.3 GHz cavities corresponds to 3 Hz detuning in 3.9 GHz cavities.

Beam loading: Similar to the above described start-to-end tracking, trajectory shift due to beam loading is considered. This scenario reflects ramping up the machine to the nominal beam current. We assume zero detuning in all cavities and compare the trajectory for zero beam current to that with a beam current of 300 μA (cf. Eq. (2)). The maximum absolute trajectory shift is 141 μm , whereas the relative trajectory shift at the end of the linac is 163 % of the beam size and can be suppressed by a trajectory feedback.

CONCLUSION

Microphonic cavity detuning related coupler kick variations affect the beam trajectory at LCLS-II. A high precision TW field map was used for tracking in the injector module and for calculating discrete coupler kicks in the main linac. Results indicate that for the expected rms detuning of 1.7 Hz coupler kick variations are well below the LCLS-II jitter tolerance of 10 %. The trajectory shift due to beam loading induced coupler kick variations during ramp up are below 141 μm and can be suppressed by a trajectory feedback.

ACKNOWLEDGMENTS

Work supported by the Department of Energy under Contract No. DE-AC02-76SF00515.

REFERENCES

- [1] G. Marcus and T. Raubenheimer, “LCLS-II: A CW X-ray FEL Upgrade to the SLAC LCLS Facility”, *ICFA Beam Dyn. Newslett.*, 70:82–102, 2017.
- [2] P. Emma *et al.* “First lasing and operation of an angstrom-wavelength free-electron laser”, *Nat Photon*, 4(9):641–647, 09 2010.
- [3] B. Aune *et al.* “Superconducting tesla cavities”, *Phys. Rev. ST Accel. Beams*, 3:092001, Sep 2000.
- [4] J. Sekutowicz, “Higher order mode coupler for TESLA”, DESY, Hamburg, Germany, Rep. DESY TESLA 94-07, 1994.

- [5] C. Adolphsen *et al.*, Modified TTF3 Couplers for LCLS-II. in *Proc. 17th Int. Conf. on RF Superconductivity (SRF'15)*, Whistler, BC, Canada, Sep. 2015, pp. 1306–1308.
- [6] C. Hovater *et al.*, “The LCLS-II LLRF System”, in *Proc. 6th Int. Particle Accelerator Conf. (IPAC'15)*, Richmond, VA, USA, May 2015, paper MOPWI021.
- [7] T. Hellert, W. Decking, and J. Branlard, “Analysis of multi-bunch free electron laser operation”, *Phys. Rev. Accel. Beams*, 20:090702, Sep 2017.
- [8] C. Schmidt, “RF system modeling and controller design for the European XFEL”, PhD thesis, University of Hamburg, Germany, 2010.
- [9] T. Hellert and M. Dohlus, “Detuning related coupler kick variation of a superconducting nine-cell 1.3 GHz cavity”, *Phys. Rev. Accel. Beams*, 21:042001, Apr 2018.
- [10] W. Ackermann, H. De Gersem, and T. Weiland, “Eigenvalue Calculations Based on the Finite Element Method With Physically Motivated Field Smoothing Using the Kirchhoff Integral”, in *Proc. 8th Int. Particle Accelerator Conf. (IPAC'17)*, Copenhagen, Denmark, May 2017, paper WEPIK064.
- [11] Link to 3D field map of the TESLA cavity, 2018: http://www.desy.de/fel-beam/s2e/data/TESLA_2018/.
- [12] T. Schilcher, “Vector Sum control of pulsed accelerating fields in Lorentz Force Detuned Superconducting Cavities”, PhD thesis, University of Hamburg, Germany, 1998.
- [13] M. Dohlus *et al.*, “Numerical Investigations Of Waveguide Input Couplers For The TESLA Superstructure”, in *Proc. 7th European Particle Accelerator Conf. (EPAC'00)*, Vienna, Austria, Jun. 2000, paper TUP5B03.
- [14] L.-Q. Lee, Z. Li, C. Ng, and K. Ko, “Omega3P: A Parallel Finite-Element Eigenmode Analysis Code for Accelerator Cavities”, Stanford, CA, USA, Rep. SLAC-PUB-13529, 2009.
- [15] J. F. Schmerge *et al.*, “The LCLS-II Injector Design”, in *Proc. 36th Int. Free Electron Laser Conf. (FEL'14)*, Basel, Switzerland, Aug. 2014, paper THP042, pp. 815–819.
- [16] Y. Nosochkov, P. Emma, T. Raubenheimer, and M. Woodley, “Development of the LCLS-II Optics Design”, in *Proc. 7th Int. Particle Accelerator Conf. (IPAC'16)*, Busan, Korea, May 2016, paper MOPOW048.
- [17] H. Wiedemann, *Particle Accelerator Physics*, vol. 3, Springer, Berlin, 2007.
- [18] I.V. Gonin, T.N. Khabiboulline, A. Lunin, and N. Solyak, “Simulations of 3.9 GHz CW Coupler for LCLS-II Project”, *Proc. 17th Int. Conf. on RF Superconductivity (SRF'15)*, Whistler, BC, Canada, Sep. 2015, pp. 1066–1069.